Check for updates

Experimental Investigation of Flow-Structure Interaction of a Compliant Panel under Mach 2 Compression-Ramp Interaction

Yoo-Jin Ahn[1], Marc A. Eitner[2], Mustafa N. Musta[3], Sina Rafati[2], Jayant Sirohi[4], and Noel T. Clemens[5]

Department of Aerospace Engineering and Engineering Mechanics,
The University of Texas at Austin, Austin, TX, 78712, USA

This experimental study focuses on fluid-structure interaction (FSI) for a thin compliant panel under a shock/boundary layer interaction (SBLI) generated by a 2D compression ramp in a Mach 2 wind tunnel. In previous work, we have studied the FSI for this configuration using simultaneous fast-response pressure-sensitive paint (PSP) and digital image correlation (DIC). Simultaneous PSP/DIC allows for examination of the relationship between the dynamic panel displacement and surface pressure loading, respectively. Spectral analysis showed that pressure fluctuations within the interaction region and shock-foot unsteadiness tend to lock to the first mode resonant frequency of the compliant panel. The current study aims to utilize synchronous high-speed stereoscopic PIV (25 kHz) and DIC (5 kHz) techniques to better understand the coupling between the flow field and the panel displacement field. The PIV is obtained in a streamwise-spanwise plane located at 15% of the boundary layer height. Thin compliant polycarbonate panel with thicknesses of 1 mm is utilized, which has a first-mode vibrational frequency of 407 Hz. The 1 mm panel out-of-plane displacement amplitude was up to 15% of the boundary layer thickness. The analysis includes low-pass and band-pass filtering of the velocity data, including the surrogate separation line, and cross-correlation analysis between panel displacement and velocity. The results indicate a clear coupling of the panel motion and velocity field, but the spectral analysis suffers from limited time records associated with the pulse-burst laser used for PIV. Future work will focus on collecting more data to improve the statistical convergence of the results.

Nomenclature

δ_{99} = Boundary layer velocity height based on 99% free stream.
U_∞ = Freestream velocity
Re = Reynolds number
x = Streamwise coordinate
y = Wall-normal coordinate
z = Cross-stream coordinate
u = Streamwise velocity
v = Wall-normal coordinate
w = Cross-stream coordinate

---

[1] Graduate Student, Member
[2] Postdoctoral Fellow, Member
[3] Lecturer, Member
[4] Professor, Associate Fellow
[5] Professor, Fellow

I. Introduction

Fluid-structure interaction (FSI) -- which is the coupling of vibrational modes of the structure to the fluid -- is an important phenomenon that occurs on thin-walled structures of high-speed vehicles [1]. FSI can lead to structure fatigue and hence disastrous consequences for the vehicle integrity and control. FSI are particularly problematic in hypersonic flight as frictional heating leads to high-heating rates that significantly weaken panels, which leads to increased compliance. Thus, strong unsteady forcing by the pressure fluctuations generated in high-speed flight due to shock-induced turbulent separation is of particular concern for the FSI problem. FSI is expected owing to the broad spectral content of shock / boundary layers interactions (SBLIs), which can overlap the resonant vibrational modes of thin vehicle panels and thus induce significant FSIs.

Several studies have examined FSIs resulting from SBLIs that occur due to impinging shocks. Some studies have found that the mean loading on a thin structure affects the flow dynamics [2], and the flow-structure interaction affects shock-foot frequency [3]. Spottswood et al. [4]–[6] demonstrated coupling at lower frequencies between panel displacement and surface pressure fields. Related previous studies from the current group have found similar results for an FSI generated by a compression ramp SBLI positioned at the downstream end of a compliant panel [7], [8]. Recently, Varigonda et al. [9] made FSI study for impinging shock generated SBLI using simultaneous measurement of the 2D velocity field, panel surface pressure field, and panel center-span deflection. They didn't observe a noticeable change in the mean incoming boundary layer profile, mean separation extent, and the mean panel surface pressure field, which they attributed to the small degree of panel displacement. However, they did observe a larger SBLI intermittent region for the compliant panel as compared to the rigid panel, and shock oscillations occurred at the panel vibrational modes. Additionally, their cross-coherence maps showed that the panel modes enhanced the coupling of the separation shock oscillations along the spanwise direction.

This study is a continuation of research on FSI of SBLIs generated by 2D compression ramps over thin compliant panels, which was presented in Refs [7], [8], [10] and published in Ref [11]. The current work will expand upon previous work, by applying synchronous 25 kHz stereoscopic PIV and 5 kHz DIC. Particular interest is in how the panel affects the low-frequency content in the velocity fields.

II.   Experimental Set-up

A. Facility and Set-Up

The experiments were performed at The University of Texas at Austin High-Speed Wind Tunnel Laboratory. The wind tunnel is a Mach 2 blow-down facility that provides a free stream velocity of 510 ms^{-1}, stagnation conditions of 261±7 kPa and 292±5 K, and nominal run time of 30 seconds. The test section is 152 mm wide by 152 mm high by 700 mm in length. The freestream turbulence intensity is less than 1%, and freestream Reynolds number are $Re_\infty = 98 \times 10^6$ m^{-1}. The test section boundary-layer thickness (δ_{99}) at the boundary layer edge velocity of $0.99U_\infty$ is 12.5 mm. Further details of the test conditions can be found in previous studies [13], [14], [16].
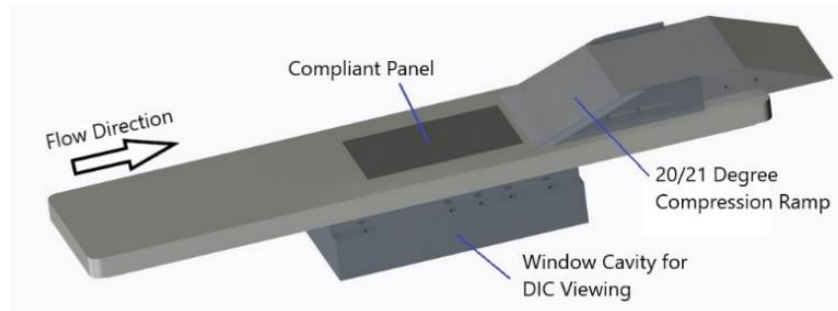
Figure 1. Schematic of the floor plug inserted into the Mach 2 tunnel floor section. The compliant panel and compression ramp are mounted to this floor plug.

This study examined a 20° compression ramp, which is 101.5 mm in width and installed spanwise-centered inside the 152 mm wide test section. The wind tunnel walls are 25 mm from the edge of the ramp, and the sidewall boundary layers are about 12 mm thick. The ramp is fitted with fences that extend 10 mm upstream of the ramp to prevent spillage and interaction with the corner vortices. The experimental models were mounted into a floor plug as shown in Figure 1. Figure 1 shows that the compliant panel is installed flush with the test section floor, and the compression ramp corner is placed at the downstream edge of the panel.

A sealed window cavity, also shown in Fig. 1, was fitted below the compliant panel to enable control over the pressure on the underside of the compliant panel. Typically, the cavity pressure is set to be same as the freestream static pressure to minimize the static deflection of the panel, but since the SBLI leads to a non-uniform pressure distribution over the surface, there is no single cavity pressure that gives zero static deflection. The windowed cavity allows an unobstructed view of the back surface of the compliant panel for digital image correlation (DIC).

A thin compliant panel was made from polycarbonate. The panel has a dimension of 127 x 68.5 mm with thicknesses of 1 mm. The panel was machined from a single thick (25 mm) block, and retains flanges to provide rigid support around the edges of the panel. The first three mode frequencies were calculated for all panels [12] and measured using impact tests and tabulated on table 1 below. However, the mode frequencies can vary up to ±100 Hz depending on the back pressure of the panel inside the cavity unit, as the mean deformation induced by the pressure difference changes the effective stiffness of the panel [17].

Table 1. Calculated [12] and measured frequencies of the first three modes

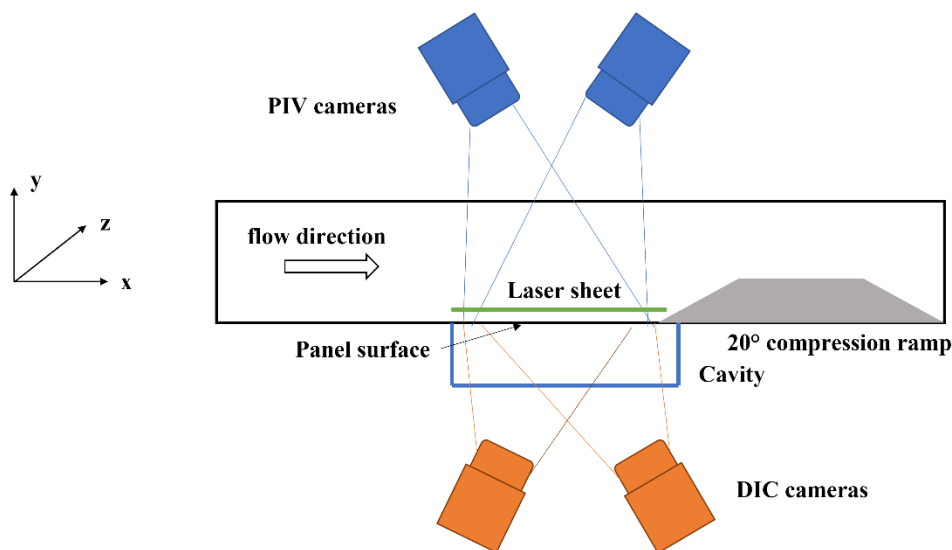| Thickness [mm]	Mode 1 [Hz]	Mode 2 [Hz]	Mode 3 [Hz]
1	349 (407)	473 (542)	675 (N/A)

Figure 2. Experimental for simultaneous PIV and DIC.

B. High-Speed Digital Image Correlation

Stereoscopic digital image correlation (DIC) allows the assessment of the 3D surface deformation of the compliant panel. The DIC system uses two high-speed cameras (Vision Research Phantom Miro M310) to obtain full three-dimensional displacement fields on a compliant panel (labeled DIC Cameras in Figure 2). The cameras were recorded at 5 kHz. A random speckle pattern is applied to the back of the compliant panel, which the system views from under the tunnel through the windowed cavity. The transient deformation of the panel is detected by imaging the change in speckle pattern. Images are then processed through LaVision DaVis v10.1 for stereoscopic digital image correlation, by setting an interrogation window size of 31×31 pixels with 7-pixel overlap.
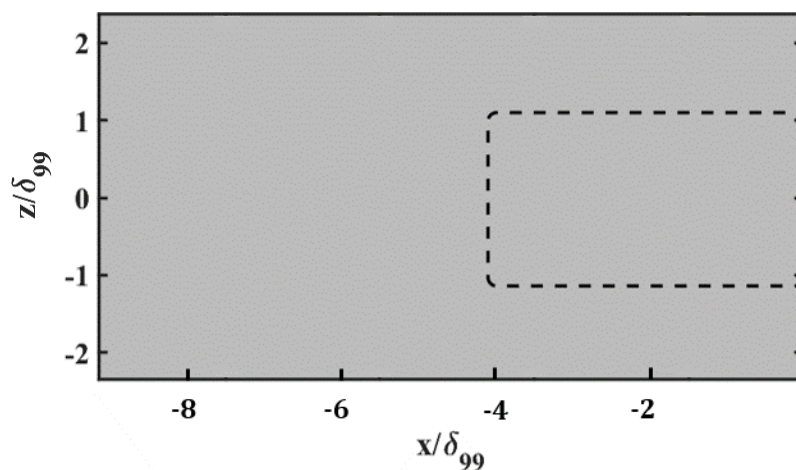

Figure 3. DIC and PIV fields of view. DIC is imaging the entire panel (gray area). PIV system is viewing the area marked by dashed rectangle. (The ramp is located on the furthest right side.)

C. High-Speed Stereoscopic Particle Image Velocimetry

The high-speed (25 kHz) stereoscopic PIV system uses two Fastcam SA-Z cameras (labeled PIV Camera in Figure 2). Each camera was angled at 13° and Schiempflug adaptors were used to view the same field of view. The field of view is shown in Figure 3. The PIV was conducted in the streamwise (x) – spanwise (z) plane. The cameras were operated at a rate of 50kHz with a resolution of 896×448 pixels. An Nd:YAG frequency-doubled pulse-burst laser (Spectral Energies 'QuasiModo') is used to produce the laser sheet. The laser produces 10.5 ms bursts of evenly spaced pulse-doublets (1500 ns apart) at 25 kHz with a center wavelength of 532 nm. The laser sheet produced was approximately 1.7 mm thick and it was introduced to the test section, parallel to the floor, approximately 2.5mm above the panel surface. Titanium dioxide (TiO_2) seeding particles were used with a primary particle size of 20 nm. The particles were seeded using a fluidized bed followed by a cyclone separator to extract the smallest particles. LaVision DaVis v8.4 was used to process the PIV images, using a multipass, adaptive interrogation scheme with an automatically adapting Gaussian weighted sub-pixel interpolation and a final window size of 32x32 px with a 50% overlap. The spatial resolution was approximately 0.05mm per pixel and 1.8mm per window.

III.   Results

A. Previous Work

Our previous work examined the dynamics of the fluid-structure interaction generated by a 2D compression ramp over a compliant panel by using simultaneous high-speed digital image correlation (DIC) and pressure-sensitive paint measurements (PSP) [7], [8], [10], [11], [16-18]. Initial experiments were made using polycarbonate thin panels with different thicknesses [7], [8], [10], [11]. It was shown that the coupling between the thin panel and first mode is dominant, which was revealed by spectral comparison between structural displacement and pressure fields on several locations of the panel surface, including shock foot motion as inferred from the surface pressure. The first vibrational mode frequency was dominant in both the pressure field and displacement fields. More detailed experiments were made using various thickness brass panels in the same facility [16-17]. From the deformation gradients in the streamwise directions, the surface pressure fluctuations were predicted using linearized potential flow theory, and these predictions were consistent with the PSP measurements.

Additional experiments were made to investigate the FSI using the 1-mm thickness polycarbonate panel, which includes the pressure measurement of the ramp surface [18]. A comparison of the spectral content between rigid and compliant panels revealed that, over the panel and ramp, there is apparent evidence of coupling of the pressure field to the panel vibratory response. This observation indicates that the shear layer reattachment process is coupled with the panel vibration. The cross-correlations between displacement and pressure fields in the upstream and separation regions showed higher magnitude than the intermittent region (shock foot) cross-correlations. Although the spectral content of the shock-foot motion showed a peak at the first mode of the panel (~400Hz), the correlation coefficient was ~0.25, which showed a weak correlation. Furthermore, full-field analysis using the spectral POD method and bandpass filtered data around structural modes agree well on the nature of the mode shapes inferred from the displacement and pressure data.

B. 25 kHz velocity fields from stereoscopic PIV

Figure 4 shows the time sequence of the instantaneous velocity fields (1mm compliant panel) obtained using 25 kHz stereoscopic PIV. The three components of velocity are shown: streamwise (U), transverse (V) and spanwise (W). The flow is from left to right and the ramp is at the right edge of the image. The velocity contours have been normalized with respect to the freestream velocity, U_∞. The interpretation of the U velocity component is straightforward: the red/dark red is the freestream region, the

yellow to green in transition to the separated flow, the aqua can be thought as the surrogate separation line and the blue is near the ramp edge. As reported from the previous studies in this facility [13], the large-scale streamwise "superstructures" are clearly present in the incoming upstream boundary layer – red bands in Figure 4(a).

Figure 5 compares V-velocity time series extracted from the upstream boundary layer (Fig. 5(a)) and the within the separated flow (Fig. 5(b)). This figure shows that in the upstream boundary layer, the magnitude of V is typically less than 5% of the freestream velocity. However, in the separation region, the out-of-plane velocities are significantly higher, with fluctuations in V reaching 80% of the freestream velocity. The W component of the velocity field shows a similar trend; a large amplification in the velocity fluctuations are seen within the separation region.

We are looking for coupling between the flow and the structural vibration, but the turbulence occurs at higher frequencies and we expect it to be largely uncorrelated to the panel motion. For this reason, the velocity field was band-pass filtered using the 3rd order Butterworth filter between 300 Hz and 2000 Hz. The low frequency bound was to remove the breathing motion of the separated region, which we also do not expect to couple to the panel vibration. Low-pass filtering the velocity data also has the advantage that it greatly reduces the effect of aliasing on the observed velocity fields.

C. Deformation field from stereoscopic DIC

Figure 6 shows the mean deformation of the 1 mm compliant panel. The direction of the deformation is perpendicular to the panel surface. Negative values indicate downward displacements of panel, that is, the panel bulges outside of the test section. In the same sense, positive deformation implies the compliant panel bulges into the test section. Figure 6 shows that during the run, the panel is significantly bulged outward at the downstream section due to the high-pressures associated with the compression ramp. For the purposes of the current study, we are concerned with dynamic coupling of the panel vibration to the flow, and from now on we will consider panel deformation where the mean has been subtracted. The data set was then high-pass filtered above 200 Hz using the 7th order Butterworth filter to eliminate very low frequency content such as vibration of the camera support structure.
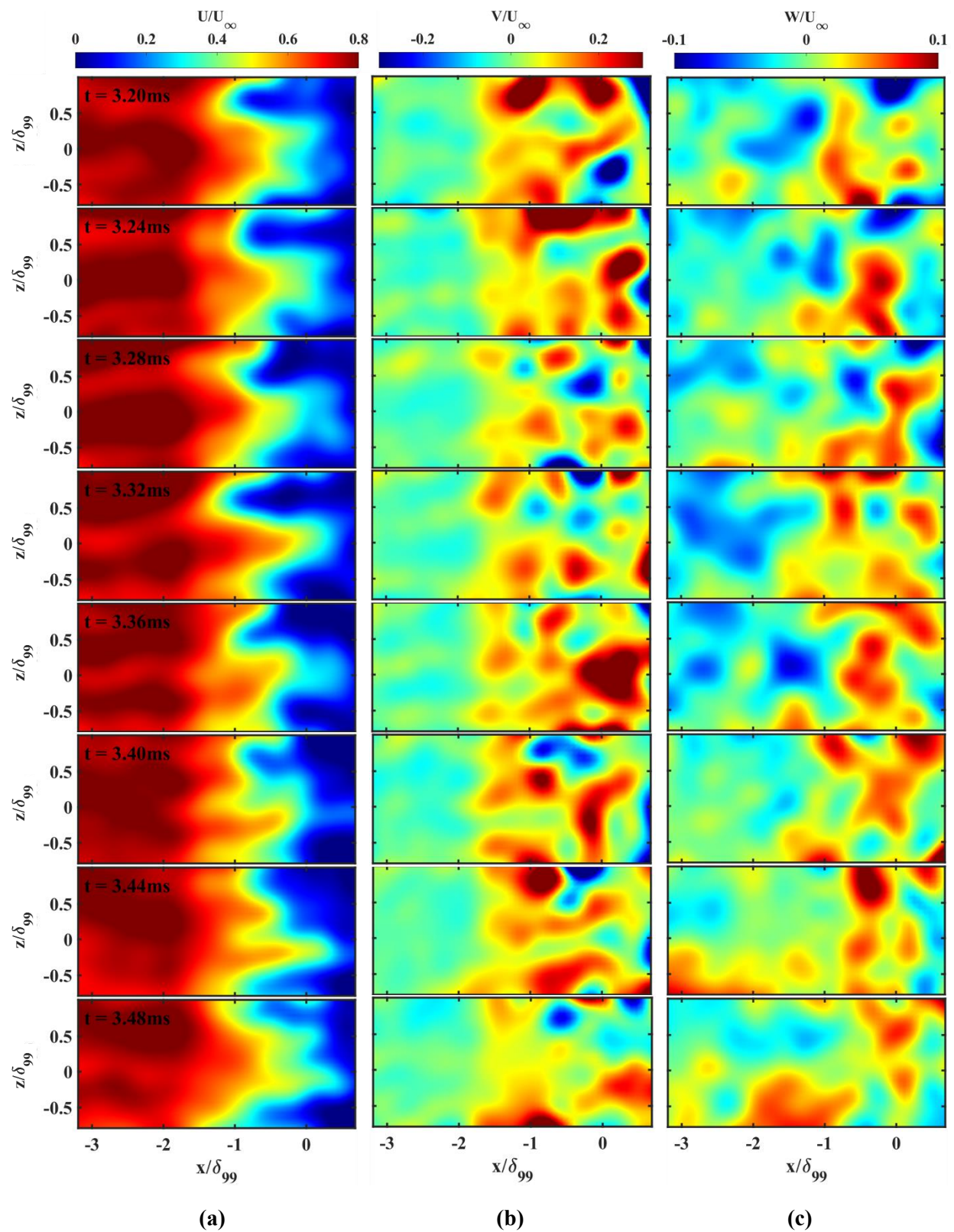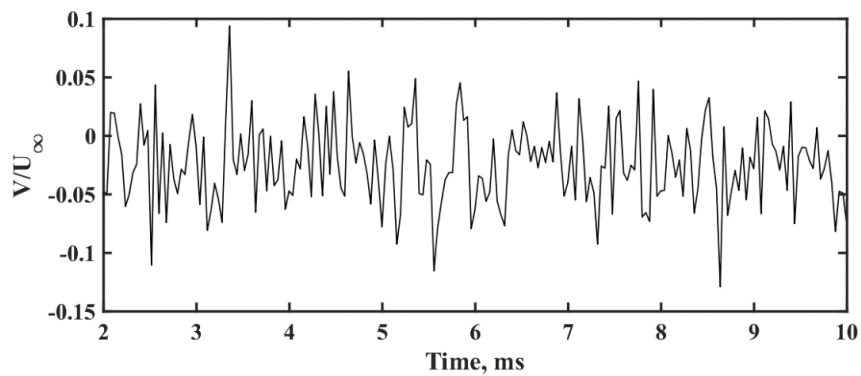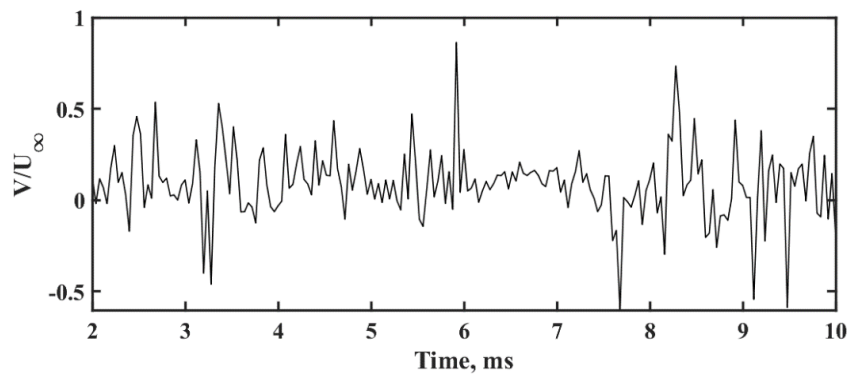
Figure 4. Unfiltered PIV velocity field normalized by the freestream velocity a) U velocity contour b) V velocity contour c) W velocity contour (The ramp is located on the furthest right side)

(a) Upstream flow region

(b) Separated flow region

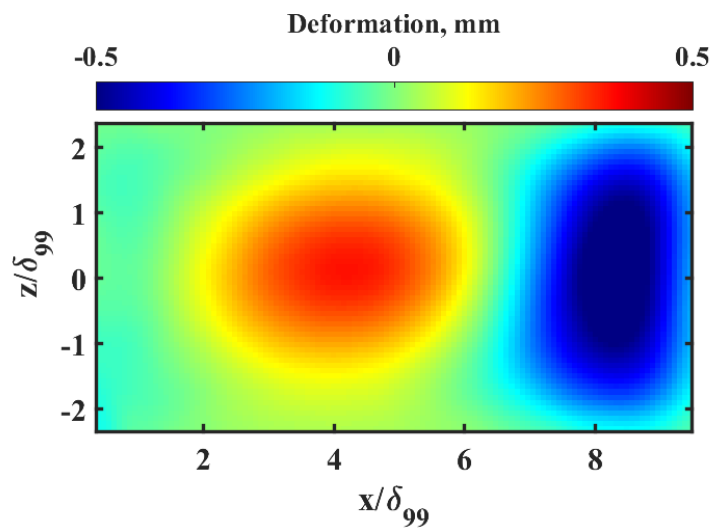**Figure 5. Normalized V velocity in time at different flow regions**

Figure 6. Mean y-displacement field. The flow is left to right and the ramp is located on the furthest right edge of the image.

The deformation power spectrum of a spatially averaged 5x5 px window on the 1 mm compliant panel is shown in Figure 7. The power spectrum was computed using Welch's method, which uses Hamming windowing. To compute the spectra, the total record of 10,000 data points was divided into subsets of 1000 points, with 50% overlap. The red dashed line is drawn at the first mode frequency, which is approximately 449 Hz; the blue dash line is at the second mode frequency around 664 Hz. These frequencies are approximately 100 Hz higher than the modal analysis results from the impact test (Table 1). The discrepancy between the impact test and wind tunnel tests is expected since the pressure loading (Fig. 6) can changes to the effective stiffness of the panel [17].

D. Correlation of a Compliant Panel with the Velocity Field

Figures 8 shows a time sequence of the mean subtracted DIC results and three velocity components of the band-pass filtered PIV. In the provided sequence, the panel deformation undergoes half a cycle: it is bulged into the test section at t = 2.60 ms (Figure 8(a)), and then moves out of the test section until it is bulged out at t = 3.40 ms (Figure 8(a)).

The velocity time sequence reveals elongated structures in the U-velocity, particularly in the upstream boundary layer. The V velocity is low in the upstream boundary layer, as discussed above, and the structures are smaller-scale with high magnitude in the separated flow region. The W velocity component is also spotty, but the scale of the structures is larger than for the V-velocity. Since the V-velocity is most likely to be affected by the direct panel motion, the spotty nature of the structures may be surprising; however, the actual velocity of the panel is just a few meters per second, and so its influence on the velocity field may still be masked by turbulence even for the low-pass bandpass filtered data.

The cross-correlation between the out-of-plane panel displacement and the velocity (V component) was also investigated. As mentioned above, the V-component is expected to have a larger correlation to the panel motion since the panel's motion is also in the transverse direction. Both values were collected at the location $2.3\delta_{99}$ upstream of the compression ramp. Since the two data sets have different sampling rates, the DIC result was up-sampled to 25 kHz using Spline interpolation. For the purpose of comparison, the velocity was high-pass filtered at 5 kHz. As expected, since low-frequency motions are filtered out, Figure 9(a) shows there is no correlation between the displacement with the high-pass filtered PIV data. However, when the velocity is low-pass filtered at 2 kHz, Figure 9(b) shows there exists a clear correlation between the deformation and the velocity fields: the correlation coefficient of 0.55 with a lag of 0.2 ms. Although there is a lag between two signals, the 0.2 ms lag may have been due to the phase change induced by the low-pass filter.
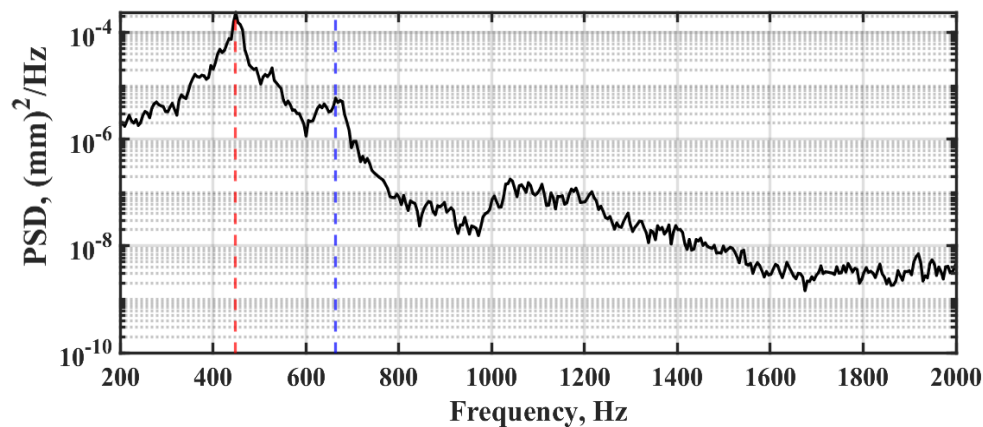
Figure 7. Power spectrum indicating the first two mode frequencies of the 1mm compliant panel
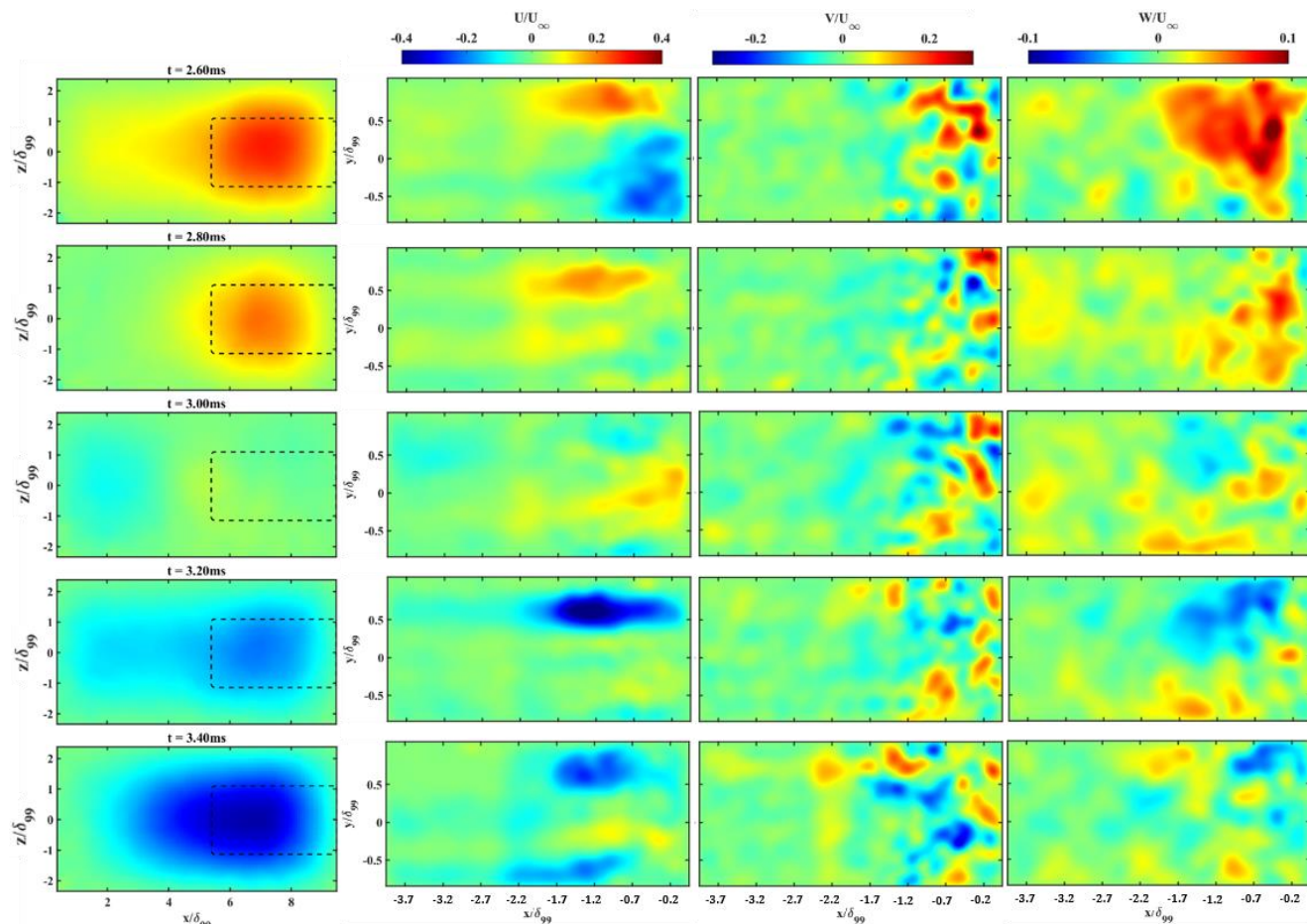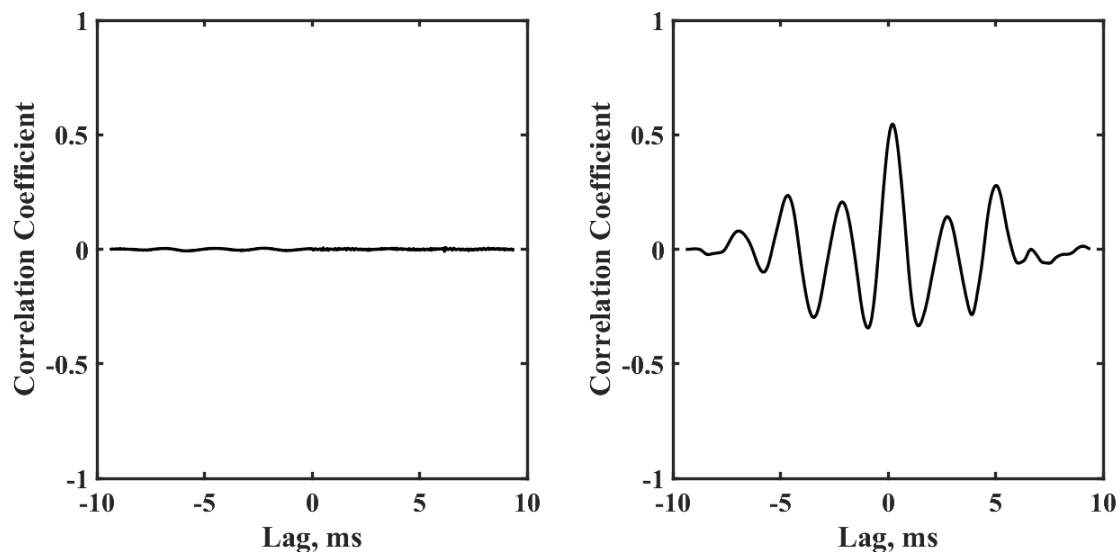

Figure 8. Time series of the mean-subtracted deformation (the first column) and the band-pass filtered (300 – 2000 Hz) velocity contours (The ramp is located on the furthest right side)

(a) DIC – high-pass filtered PIV (above 5 kHz) (b) DIV – low-pass filtered PIV (below 2 kHz)

Figure 9. Cross-correlation between the out-of-plane displacement and the V velocity

E. Coupling of the Panel Displacement with the Surrogate Separation Line

Figure 10 shows the sequence of the U velocity contour with the surrogate separation line marked as a red line. The surrogate separation line was identified using the threshold method; an arbitrarily low velocity of 30% of the freestream velocity was chosen as the threshold. The change in the streamwise location of the separation line around $y/\delta_{99} = 0$ was then recorded.
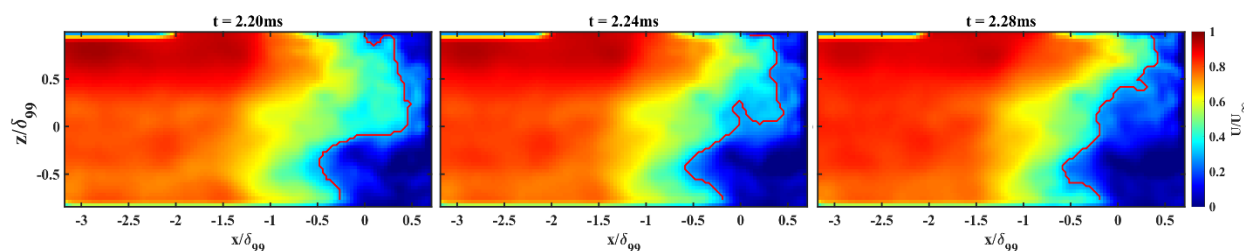

Figure 10. Normalized U velocity contour with the surrogate separation line marked in red line

Figure 11 shows frequency normalized power spectra of the surrogate separation line location fluctuations. The rigid panel case is also shown to provide a baseline (Figure 11(a)). The power spectra were obtained using Welch's method. A Hamming window with the same length of the data was used with 50% overlap. It should be noted that due to the limitation in the duration of the pulse-burst laser (10.5 ms), the PIV data time record extends over only about 5 cycles of the first vibrational mode of the panel. As a result, the spectra are not converged and should be viewed with caution. Our future work will focus on gathering multiple pulse-bursts to improve the quality of the statistical results. With this concern in mind, Fig. 11(b) shows the power spectrum of the separation line surrogate for the rigid case exhibits two peaks, one at 292 Hz and the other near 1100 Hz. It is not clear why the surrogate separation line exhibits peaks at these two frequencies, or whether such peaks are associated with our particular wind tunnel. However, a

comparison to the compliant panel case does show some differences. In particular, the compliant panel shows a large peak near 650 Hz, which seems to be related to the second vibrational mode. There is also a smaller peak near the first-mode frequency, but we would need more data to know if this peak is tied to the panel motion. This observation that the surrogate separation line may be oscillating at the second mode frequency seems to disagree with the simultaneous PIV/PSP results reported in [18], as they showed strong coupling between the separation shock foot motion and the first vibrational mode. We expect the shock foot and separation line to be coupled in their motions and so the reason for this discrepancy is not clear at this time.
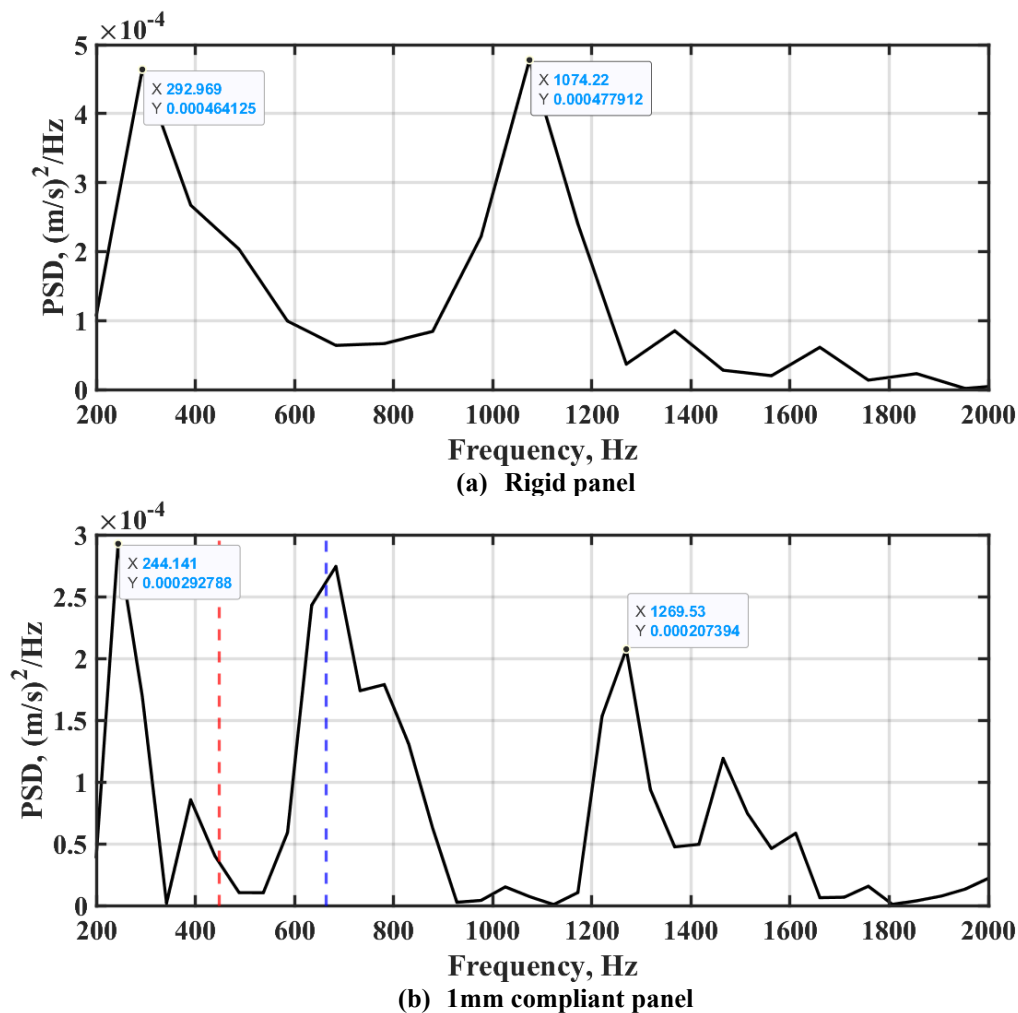

(a) **Rigid panel**

(b) **1mm compliant panel**

Figure 11. Power spectra of the x-location change in the surrogate separation line

IV.   Conclusion

In this study, FSI of a 1 mm compliant panel has been studied using simultaneous high-speed DIC and PIV. The DIC was acquired at 5 kHz and the PIV at 25 kHz. The mean-subtracted deformation field and the band-pass filtered velocity fields have qualitatively shown that there is a potential coupling between the low-frequency panel movement and the velocity field. We found a noticeable correlation between the panel displacement and the transverse (y-direction) velocity fluctuations. The power spectrum of the surrogate separation line location further seems to indicate some level of coupling between two fields,

although these results should be viewed with caution owing to poor statistical convergence. Previous FSI research conducted in this facility has also utilized the fast-response PSP with DIC. The spectral comparison between pressure fields of the compliant and rigid panels indicates that there is coupling between the panel movement and the surface pressure at the first and second modal frequencies of the panel. The future experimental work will focus on acquiring more pulse-bursts to enable better statistical convergence of the results. Also, future work will include simultaneous high-speed DIC, fast-response PSP, and high-speed PIV based upon this preliminary research. The combined deformation, pressure, and velocity measurements are expected to further unveil the mechanism behind flow-structure interaction.

V. Acknowledgments

References

[1]   J. J. McNamara and P. P. Friedmann, "Aeroelastic and Aerothermoelastic Analysis in Hypersonic Flow: Past, Present, and Future," *AIAA J.*, vol. 49, no. 6, pp. 1089–1122, 2011, doi: 10.2514/1.J050882.

[2]   S. Willems, A. Gülhan, and B. Esser, "Shock induced fluid-structure interaction on a flexible wall in supersonic turbulent flow," vol. 5, pp. 285–308, 2013, doi: 10.1051/eucass/201305285.

[3]   L. Maestrello and T. L. J. Linden, "Measurements of the response of a panel excited by shock boundary-layer interaction," *J. Sound Vib.*, vol. 16, no. 3, pp. 385–388, 1971, doi: 10.1016/0022-460X(71)90594-3.

[4]   S. M. Spottswood, T. Eason, and T. Beberniss, "Full-field, dynamic pressure and displacement measurements of a panel excited by shock boundary-layer interaction," May 2013, doi: 10.2514/6.2013-2016.

[5]   S. M. Spottswood *et al.*, "Exploring the response of a thin, flexible panel to shock-turbulent boundary-layer interactions," *J. Sound Vib.*, vol. 443, pp. 74–89, 2019, doi: 10.1016/j.jsv.2018.11.035.

[6]   S. M. Spottswood, T. Eason, and T. Beberniss, "Influence of shock-boundary layer interactions on the dynamic response of a flexible panel," *Proc. Int. Conf. Noise Vib. Eng. ISMA 2012*, pp. 603–616, 2012.

[7]   T. J. Goller, M. Musta, D. Uehara, J. Sirohi, and N. T. Clemens, "Experimental Study of a Compliant Panel under a Mach 2 Compression Ramp Interaction," , *71st Annual Meeting of the APS Division of Fluid Dynamics,* 2018.

[8]   T. J. Goller, M. Musta, L. Vanstone, N. T. Clemens, L. Mears, and J. Sirohi, "Simultaneous High-Speed Displacement and Surface Pressure Measurements of a Compliant Panel under a Mach 2 Compression Ramp Interaction," *Presented in AIAA SciTech Invited Session*, 2019.

[9]   S. V. Varigonda, V. Narayanaswamy, and I. Boxx, "Investigations of fsi generated by an impinging sbli on a thin panel using multivariate imaging of flow/structural properties," *Aiaa Aviat. 2020 Forum*, vol. 1 PartF, pp. 1–20, 2020, doi: 10.2514/6.2020-3001.

[10]   M. Musta, L. Vanstone, M. Eitner, J. Sirohi, and N. T. Clemens, "A Compression - Ramp Shock/Boundary-Layer Interaction Over a Compliant Panel at Mach 5," , *72nd Annual Meeting of the APS Division of Fluid Dynamics* ,2019.

[11]   M. Eitner, M. Musta, L. Vanstone, J. Sirohi, and N. Clemens, "Modal Parameter Estimation of a Compliant Panel Using Phase-based Motion Magnification and Stereoscopic Digital Image Correlation," *Exp. Tech.*, pp. 287–296, 2020, doi: 10.1007/s40799-020-00393-6.

[12]   L. Vanstone and N. T. Clemens, "Structure and Unsteadiness of Swept-Ramp Shock Wave/Turbulent Boundary Layer Interactions," in *31st International Symposium on Shock Waves 1*, 2019, pp. 81–93, doi: 10.1007/978-3-319-91020-8_8.

[13]   B. Ganapathisubramani, "Statistical properties of streamwise velocity in a supersonic turbulent boundary layer," *Phys. Fluids*, vol. 19, no. 9, p. 098108, 2007, doi: 10.1063/1.2772303.

[14]   L. Vanstone, M. N. Musta, S. Seckin, and N. Clemens, "Experimental study of the mean structure and quasi-conical scaling of a swept-compression-ramp interaction at Mach 2," *J. Fluid Mech.*, vol. 841, pp. 1–27, Apr. 2018, doi: 10.1017/jfm.2018.8.

[15]   B. Ganapathisubramani, N. T. Clemens, and D. S. Dolling, "Low-frequency dynamics of shock-induced separation in a compression ramp interaction," *J. Fluid Mech.*, vol. 636, pp. 397–425, 2009, doi: 10.1017/S0022112009007952. [1] T. J. Goller, D. U. Mustafa N. Musta, Leon Vanstone, and N. T. C. Lee Mears, Jayant Sirohi, "Simultaneous High-Speed Displacement and Surface Pressure Measurements of a Compliant Panel under a Mach 2 Compression Ramp Interaction,", *Presented in AIAA SciTech Invited Session*, 2019.

[16]   M. A. Eitner, "Experimental Investigation of Fluid-Structure Interaction of a Compliant Panel under a Mach 2 Compression Ramp Shock-Boundary Layer Interaction," Ph.D. Thesis, the University of Texas at Austin, 2021.

[17]   M. Eitner, Y. Ahn, M. Musta, L. Vanstone, J. Sirohi and N. Clemens, "Effect of Shock Wave Boundary Layer Interaction on VibratoryResponse of a Compliant Panel," in *AIAA Aviation Forum-2493*, 2021.

[18]   M. Musta, L. Vanstone, Y. Ahn, M. Eitner, J. Sirohi and N. Clemens, "Investigation of flow-structure coupling for a compliant panel under a shock/boundary-layer interaction using fast-response PSP," in *AIAA Aviation Forum-2809,* 2021.